Ventilation Performance of Office Building with Natural Ventilation Shaft

Toshihiko Sajima[1], Eunsu Lim[*2], Toshio Yamanaka[1],
Iwao Hasegawa [3], and Akihiro Matsumoto [3]

1 Osaka University
Suita 565-0871
Osaka, Japan
**sajima_toshihiko@arch.eng.osaka-u.ac.jp*

2 Toyo University
Kawagoe 350-8585
Saitama, Japan
**lim@toyo.jp*

3 NIKKEN SEKKEI LTD
Chiyoda 102-8117
Tokyo, Japan

ABSTRACT

Using natural ventilation is effective to save energy, and it is essential for energy conservation and decreasing running cost *[1]*. However, in office buildings located in where mid- to -high-rise buildings are densely distributed, the way of ensuring stable ventilation is very important matter of natural ventilation system. In this research, we focus on the ventilation performance of an office building where the natural ventilation system is introduced by utilizing the buoyancy force through a ventilation shaft. First, the air change rate (ACH) of target rooms were estimated using CO_2 generated from occupants as tracer gas in the measurement that was conducted in the autumn in 2017. In addition, influence of the outdoor condition on airflow rate was investigated by flow network calculation based on the wind pressure coefficient of the target building that was obtained from CFD analysis.

Since the target building is located in a densely built-up block area, wind-induced natural ventilation seems to be unstable and difficult to apply. Therefore, a natural ventilation shaft is introduced and the room air is ventilated by buoyancy. A 10-story office building was analyzed, and the natural ventilation system is introduced to 4F to 9F floors. There exist two natural ventilation shafts, one is for the lower floors (4-7 F), and the other is for the higher floors (8-9 F), to prevent the backflow from the shaft at the upper floors.

In this study, in order to understand the indoor environment and the air change rate (ACH) when natural ventilation openings are open, several kinds of measurements were conducted in the office rooms of lower floors (4F - 7F) from 5th October 2017 to 8th November 2017. In the measurement, the following measurements were conducted, **(a)** CO_2 concentration, temperature, and humidity in the indoor occupied area, **(b)** pressure difference at the natural ventilation shaft, **(c)** number of people existing in the room by the observation camera. The amount of CO_2 generated per person in the room was first estimated when the mechanical ventilation was operated. Then, the air change rate (ACH) was obtained during natural ventilation as well.

By estimating the airfow rate, the air change rate (ACH) of the target room for each floor was found to be 1.0 to 2.5[1/h]. In addition, based on the pressure difference measurement at the natural ventilation shaft, it was observed that the outdoor air occasionally flows backward from the shaft to the office room despite that it was assumed to be an exhaust path. This is because the temperature inside the shaft has not sufficiently increased. Then correlation between airflow rate and the following outdoor condition v, Δt_r, Δt_s (external wind speed, temperature difference between indoor and outdoor air, temperature difference between outside and the inside the shaft) was calculated, and Δt_r showed the greatest correlation. In the target building, it was found that Δt_r (the difference between the indoor and outdoor temperature) was the main driving force.

In order to calculate the airflow rate by flow network model, CFD analysis assuming a model experiment in the wind tunnel was conducted to obtain the wind pressure coefficient in the 8 wind direction. As a result of calculation of airflow rate by the flow network model changing the outside air temperature and the external wind, the backflow from the shaft to the office room was seen in some wind direction. However, no backflow occurred when temperature difference between indoor and outdoor air was large. It is a challenge to ensure a sufficient temperature difference within the shaft to achieve stable ventilation.

KEYWORDS

Natural Ventilation Shaft, Field Measurement, Tracer Gas, Airflow Rate, Flow Network Calculation

1 INTRODUCTION

In an office building located in Tokyo, Japan where mid- to high-rise buildings are dense, it is difficult to obtain a sufficient space for ventilation route and solar radiation. Therefore, it is a challenge for natural ventilation (hereinafter referred to as NV) systems to ensure stable

ventilation in such a site. In order to solve these problems, it is indispensable to conduct both experimental approach and analysis of operational data of NV systems. Hasegawa *[2]* investigated NV performance of the building completed in September 2012(H Building, Existing Building). In this research, the authors aim to evaluate the ventilation performance of an office building with NV shaft. In this paper, we investigate the NV performance of the office building (H Building, Extension Building) completed in March 2017 on the southeast side of the existing building. The airflow rate was comprehended by tracer gas method and flow network calculation. First, on-site measurement was carried out in the autumn of 2017, and when the NV was operated, the airflow rate was measured using CO_2 generated from occupants as a tracer gas. Secondly, the wind pressure coefficient was obtained by CFD analysis, which was used to calculated the airflow rate by flow network calculation. Then, the effect of outdoor condition on airflow rate is studied.

2 OUTLINE OF NATURAL VENTILATION SYSTEM

The outline of the target building is shown in **Table 1**, the site plan and schematic of the cross-section of the building are shown in **Figure 1** and **Figure 2** respectively. Since the target building is located in a high density area in Tokyo, Japan, it is difficult to apply wind-induced natural ventilate in the horizontal direction. Consequently, both the existing building and extension building introduce a ventilation system using a NV shaft. **Figure 3** shows the NV openings. Outdoor air is introduced through the NV openings equipped on the external wall surface of the building, and is supplied from the inlets on the ceiling surface. In the new building, the NV system is introduced to 4th to 9th floor, and two separate shafts are planned for the lower floors (4 - 7 F) and for the higher floors (8 - 9 F) to prevent the backflow to the office room from the shaft in the upper floor.

Table 1: Summary of target building

Summary of target building	
Location	Chuo-ku, Tokyo
Applicatio	Office building
Floor	Above-ground floor: 10F
Volume of office	588 m³
Etc.	Floor height: 4.0m, Ceiling height: 2.8m Air conditioning system: Air-cooling multi package system for building

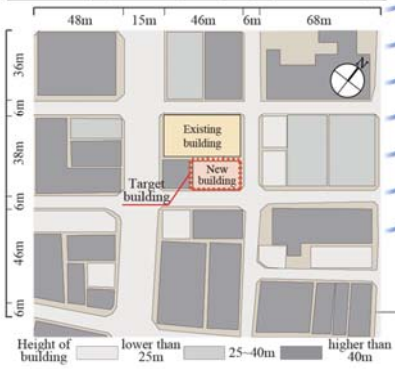

Figure1: Around the site of the building

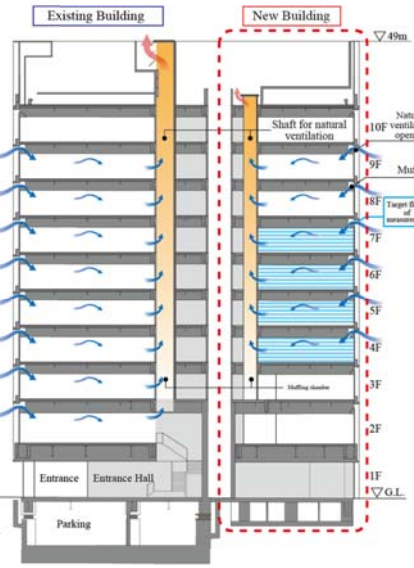

Figure 2: Sectional plan of the building

(a)Facad

(b)Inlet

Figure3: NV opening

3 EVALUATION OF VENTILATION PERFORMANCE BY MEASUREMENT

3.1 Measurement method

To understand the indoor environment and the air change rate (ACH) when NV is operated, we carried out an on-site measurement in the office room of the extension building (4 - 7F) from 5th October to 8th November 2017. **Figure 4** shows the floor plan of the target building and measurement points. In this measurement, the following items were measured.

(a) CO_2 concentration and temperature in the occupied area to evaluate the indoor environment

(b) differential pressure at the exhaust damper to confirm whether it flows out or flows in

(c) the number of occupants to estimate the amount of CO_2 generated from a person using observation camera

In the measurement of the pressure difference Δp, it was difficult to insert a pressure tubes into the shaft across the damper. Therefore pressure difference was measured at two points in the office side, and the data used for checking the airflow direction at exhaust damper.

As shown in **Figure 5**, at 7th floor, when mechanical ventilation is under operation, CO_2 concentration in the exhaust air was measured at the exhaust port of the outdoor air conditioner that was installed above the ceiling. During the measurement, if NV is judged to be valid by automatic control, the NV openings and exhaust damper are opened and the air conditioning stops, while reverse operation is performed when it is judged invalid.

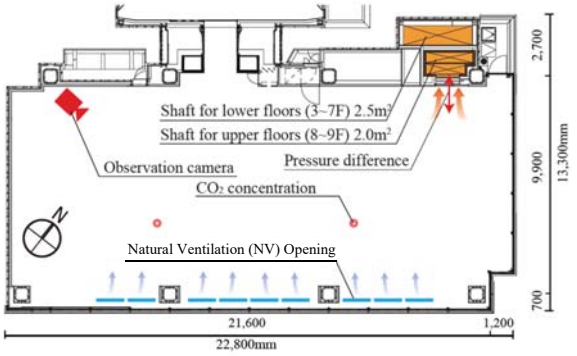

Figure 4: Floor plan of the building

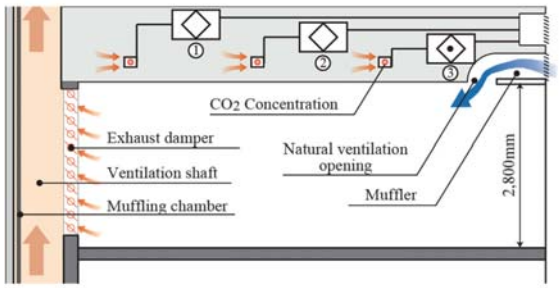

Figure 5: Sectional view of office room

3.2 Evaluation method of ventilation performance

To evaluate the amount of CO_2 generated inside the room, the CO_2 emissions per person was estimated using Equation (1). However, the estimation was performed when all three outdoor-air processing unit were operating, and the introduction amount of outside air by mechanical ventilation was set at 500 CMH for each of them.

$$M=\frac{Q}{1-e^{-\frac{Q}{V}(t-t_0)}}\{C_r-C_o-(C_{ro}-C_o)e^{-\frac{Q}{V}(t-t_0)}\} \quad (1)$$

In order to grasp the airflow rate by other than mechanical ventilation, the air change rate (ACH) by leakage was also calculated from the process of concentration decay method in the target room without occupants. For the calculation, the air change rate (ACH) was calculated by using Equation (2).

$$C_r(t)=C_o+\{C_r(t_o)-C_o\}e^{-N(t-t_0)} \quad (2)$$

Then, the airflow rate of each target room was obtained using Equation (3). Also, the airflow rate was calculated for 30 minutes after NV openings were opened for all measurement floor. The average value of the number of occupants during the 30 minutes was used to calculate the amount of CO_2 generated in the room.

$$C_r(t)=C_o+\{C_r(t_o)-C_o\}e^{-\frac{Q}{V}(t-t_0)}+\frac{M}{Q}\{1-e^{-\frac{Q}{V}(t-t_0)}\} \quad (3)$$

3.3 Results and discussion

Figure 6 shows the indoor CO_2 concentration of 6th floor during the 5 weekdays from 23th to 27th October, together with the airflow direction judged by the measurement of pressure difference. It can be seen outside air from the NV shaft backflow to the room, but when the NV window is opened, the indoor CO_2 concentration is about 500 to 600 ppm, indicating that the indoor CO_2 concentration was reduced.

Figure 7 (a) shows the frequency of outdoor and room air temperature during NV and air conditioning operation. The frequency during NV is smaller than that during air conditioning. **Figure 7 (b)** shows the frequency of outside air CO_2 concentration and room air CO_2 concentration during NV and air conditioning. During NV, indoor CO_2 concentration is distributed in 460 to 640 ppm. On the other hand, during air conditioning, indoor CO_2 concentration is distributed in 480 to 840 ppm, and it can be seen that the indoor CO_2 concentration is reduced by about 200 ppm during NV, compared with air conditioning.

Figure 8 shows the concentration decay process and the calculation results of the number of air change rate (ACH) due to the leakage of the 7F office. Under each condition, ACH is 0.072 to 0.187 [1/h], and it was shown that the airflow rate other than mechanical ventilation is sufficiently small. Assuming that the ventilation is based only on mechanical ventilation, estimation of the CO_2 emissions per person was performed.

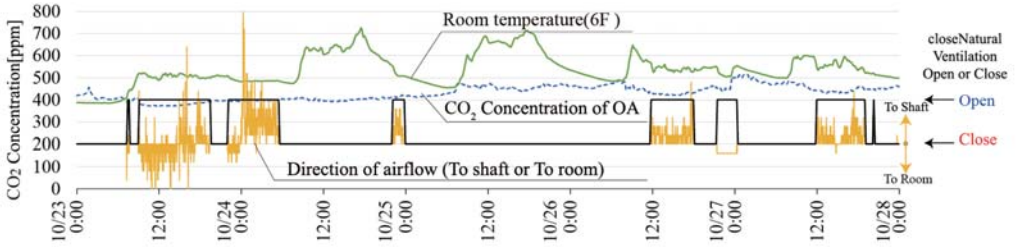

Figure 6: Operation of natural ventilation (NV) openings and CO_2 concentration (10/23 - 10/27)

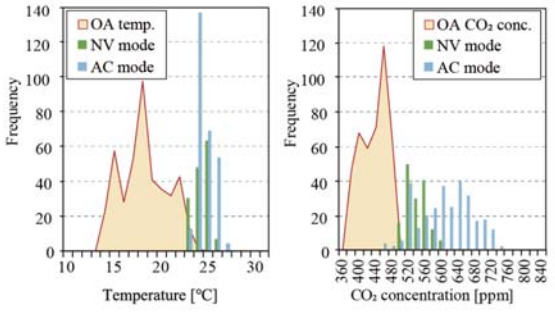

(a)Temperature (b)CO_2 Concentration

Figure 7: Frequency during each ventilation (10/23 – 10/27)

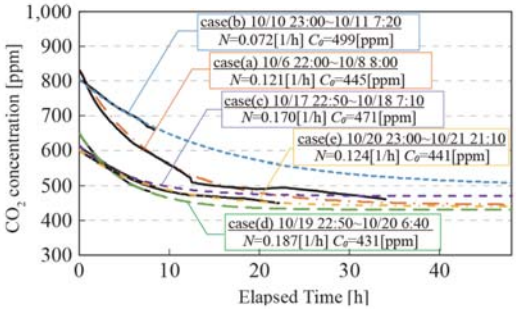

Figure 8: Concentration attenuation process

The amount of CO_2 emissions per person was calculated by equation (1) when the number of people in the room did not change for more than 1 hour. In the calculation, three outdoor-air processing units were set to 500 CMH (N = 2.3 [1 / h]) per one unit. As a result, CO_2 emissions per person were 0.0287 [m^3/h]. It is generally known that the amount of CO_2 generated during the seating office work is approximately 0.0129 to 0.230 [m^3/h] (e.g.*[3] M., Tajima, 2016)*, which is smaller than the calculation result. This may be due to that the total rate of mechanical ventilation was actually smaller than that expected to be 1,500 CMH. The influence due to the distribution is also conceivable *[4]*.

Table 2 shows the outdoor conditions and the calculation results of the air change rate (ACH) of each floor. Considering that the estimation error cannot be ignored, 0.020 [m^3/h], as a standard design value in office work, was used for CO_2 emissions per person (*[5] JIS A14061974, 2010*). **Figure 9** shows the CO_2 concentration and the number of people in the room 30 minutes after the NV openings on all floors were opened.

Figure 10 shows the air change rate (ACH), room temperature difference Δt_r (room temperature - outside air temperature), and shaft temperature difference Δt_s (shaft inside temperature - outside air temperature) for each floor.

In all of the conditions, the air change rate (ACH) of each floor is not high. This is because shaft temperature difference Δt_s is insufficient and the buoyancy force is small.

(1) Case 2 (N= 0.7 ~ 2.2 [1/h])

Indoor CO_2 concentration declined at each floor. At 5th floor, the room temperature difference Δt_r is large, so that ventilation by buoyancy force is promoted and the airflow rate of 5F is increased.

(2) Case 4 (N= 0.6 to 2.1 [1/h])

The shaft temperature difference Δt_s is small, and the room temperature difference is the main force of the ventilation. The airflow rate of the 7th floor is large, influenced by the room temperature difference and the external wind. It is believed that the indoor/outdoor temperature difference at 5th floor exceeds the influence of the external wind for 6th floor, which resulted in larger airflow rate at the 5th floor.

(3) Case 6 (N= 1.6 to 1.9 [1/h])

The room temperature difference Δt_r and the shaft temperature difference Δt_s in this case are larger than the other case, and the ventilation by buoyancy is promoted. The air change rate (ACH) is increased at all floors.

In **Figure 11**, the vertical axis represents the airflow rate, the horizontal axis represents (a) the room temperature difference, (b) the shaft temperature difference, and (c) the outside wind speed, and the results are plotted for all the 6 cases. Comparing the coefficient of determination r^2 in (a) - (c), a weak correlation is seen in (a), but no significant correlation is seen in (b), (c). Among these three parameters, the influence of indoor and outdoor temperature difference is the largest.

Table 2: Outside air condition and air change rate (ACH)

case1					
Measurement time		10/6 11:30～12:00			
Outdoor Temperature	[℃]	18.7			
Outdoor Wind Velocity	[m/s]	1.8 , N			
Wind Velocity in Shaft	[m/s]	0.70			
Air Change per Hour	[1/h]	4F	5F	6F	7F
		2.6	1.2	2.1	1.9
case2					
Measurement time		10/11 20:10～20:40			
Outdoor Temperature	[℃]	22.0			
Outdoor Wind Velocity	[m/s]	1.0 , ENE			
Wind Velocity in Shaft	[m/s]	0.65			
Air Change per Hour	[1/h]	4F	5F	6F	7F
		1.5	2.2	0.8	0.7
case3					
Measurement time		10/23 15:50～16:20			
Outdoor Temperature	[℃]	20.9			
Outdoor Wind Velocity	[m/s]	3.4 , NW			
Wind Velocity in Shaft	[m/s]	0.90			
Air Change per Hour	[1/h]	4F	5F	6F	7F
		0.8	0.9	1.4	1.8
case4					
Measurement time		10/23 18:10～18:40			
Outdoor Temperature	[℃]	19.1			
Outdoor Wind Velocity	[m/s]	1.9 , NW			
Wind Velocity in Shaft	[m/s]	0.78			
Air Change per Hour	[1/h]	4F	5F	6F	7F
		0.7	1.3	0.6	2.1
case5					
Measurement time		11/7 18:10～18:40			
Outdoor Temperature	[℃]	20.9			
Outdoor Wind Velocity	[m/s]	1.3 , SW			
Wind Velocity in Shaft	[m/s]	0.78			
Air Change per Hour	[1/h]	4F	5F	6F	7F
		1.1	1.2	1.0	1.3
case6					
Measurement time		11/8 15:20～15:50			
Outdoor Temperature	[℃]	18.8			
Outdoor Wind Velocity	[m/s]	2.6 , SW			
Wind Velocity in Shaft	[m/s]	0.50			
Air Change per Hour	[1/h]	4F	5F	6F	7F
		1.8	1.8	1.9	1.6

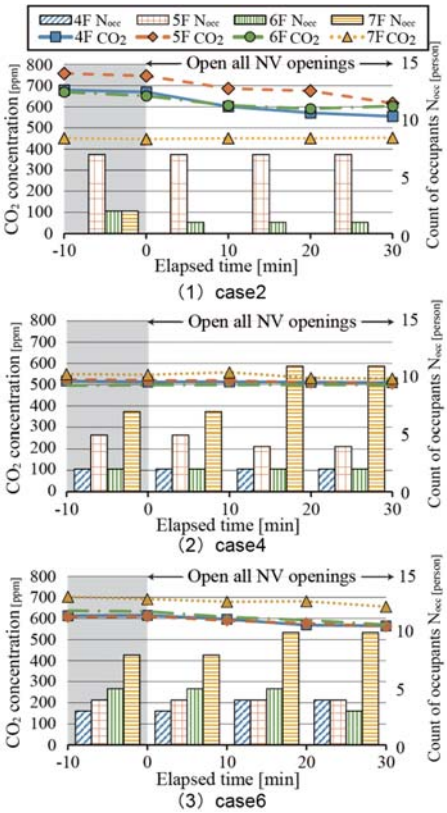

Figure 9: Indoor CO_2 concentration and number of occupants

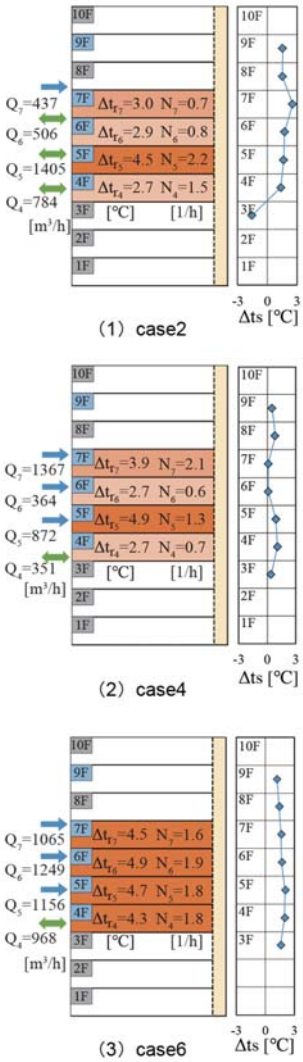

Figure 10: Airflow Rate in each floor

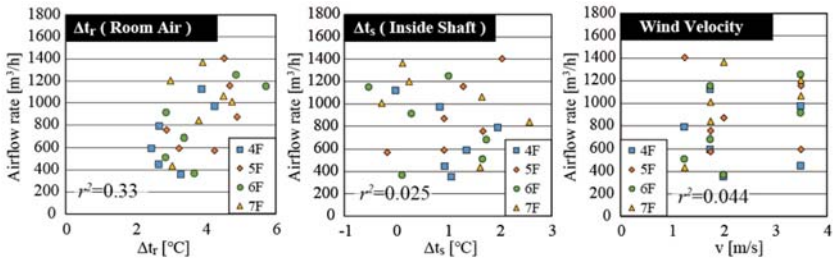

Figure 11: Correlation between outside air condition and airflow rate

4 AIRFLOW RATE ESTIMATION BY FLOW NETWORK MODEL

4.1 Wind pressure coefficient by CFD analysis

Table 3 shows the outline of CFD analysis. In this CFD analysis, the experiments at the wind tunnel (width 1,500 mm, height 1,200 mm, length 7,200 mm) are reproduced. **Figure 12** shows the computational domain and **Figure 13** shows the wind direction and building layout modeled in this analysis. The 1/300 scaled models of the target building and surrounding buildings were assumed. The CFD analysis were performed for every 45° of wind direction, and 8 cases were analyzed in total. Therefore, the wind pressure coefficient of the target building wall surface was obtained for 8cases of wind directions. The calculation points of wind pressure coefficient are shown in **Figure 14**, i.e., 29 points in total, 27 of which were located on the southeastern facade on each floor where NV openings are installed, and 2 were for the openings of the top of two shafts. As the reference dynamic pressure of the wind pressure coefficient, the dynamic pressure of the approaching flow at the target building height was adopted. Value for each height of the inflow boundary is set as the wind speed of the approaching flow according to the 1/5 power law.

Table 3: Outline of CFD analysis

CFD code	Fluent18.1
Analysis domain	7,200×1,200×1,500mm
Turbulence model	Standard k-ε model (SKE)
Algorithm	SIMPLE
Discretization Scheme	Upwind Differencing
Number of mesh	5,566,138

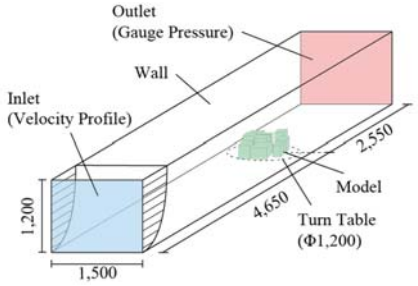

Figure 12: Analysis area

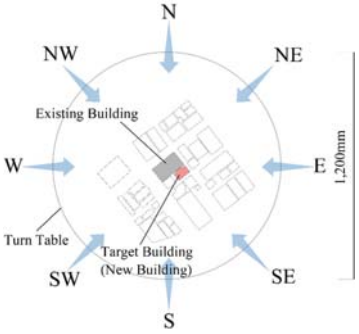

Fig 13: Modeling area and wind direction

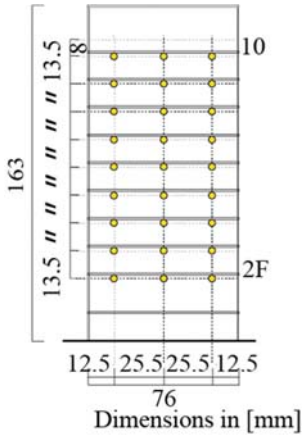

Figure 14: calculation point of *Cp*

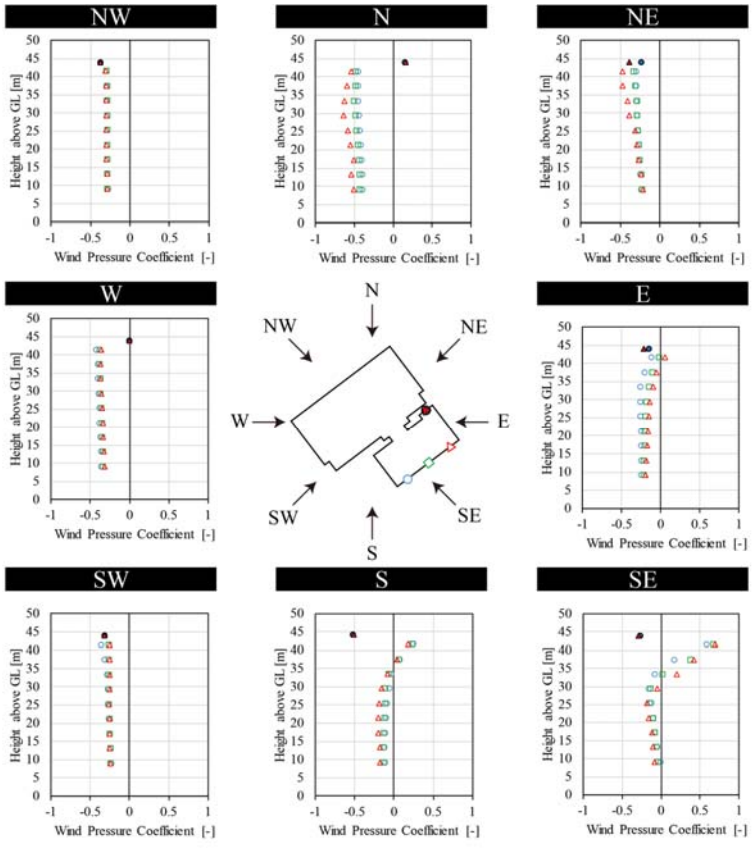

Figure 15: *Cp* Value of the model obtained from CFD analysis

Figure 15 shows the analysis results of the wind pressure coefficients on the southeastern facade of the target building. In the wind direction of SE, where the wind is approaching almost perpendicular to the wall surface, a wide range of wind pressure distribution can be seen, and the pressure becomes large at the upper part. Similar tendencies are also seen in wind direction of S and E. This is because the wind pressure became smaller at the lower part of the building due to the building at the opposite side of the street. Except these three wind directions, the difference in wind pressure coefficient between at NV opening and the top of the shaft is generally small, and the driving force of wind-induced ventilation is small, so that ventilation by buoyancy force is the main driving force of NV.

Since the opening at the top of the shaft was installed as a vertical opening on the wall surface of the NW, in the wind direction N and W, the wind pressure coefficient at the opening at the top of the shaft is larger than that of the NV opening,which can lead to the backflow from the shaft to office room when the external wind in this wind direction becomes large.

4.2 Flow network calculation model

Figure 16 shows the outline of the flow network calculation model for the office room for all floors with NV system. The calculation model has 8 spaces including six office spaces from 4th to 9th floor, and two shaft spaces for the lower and upper floors. The shaft for the lower floors is connected to the office room from 4th to 7th floor, and the shaft for the upper floors is for 8th and 9th floors. In order to express the temperature distribution, the shaft space is divided for each floor. All the office space has 4 openings including 3 NV openings and 1 exhaust opening with a damper.

The basic equation used for the flow network calculation is shown below. Calculation is performed with the room pressure in each room as the unknown, and the room pressure in each space satisfying the airflow rate balance is identified by the least squares method.

When calculating the airflow rate, the wind pressure coefficients at the NV openings and the top opening of the shaft obtained by CFD analysis are used. P_{ij} [Pa] and P_{Sj} [Pa] are the room pressure of the office space and the shaft space for each floor respectively, the reference height of the room pressure is the bottom of each space, the reference height of outside air pressure is set the bottom of the calculation model (the floor level of 4F). $h_{0,Wj}$ is the height from the outside air pressure reference height to the NV openings for each floor. h_W and h_E are the heights from the room pressure reference height to the NV openings and the exhaust

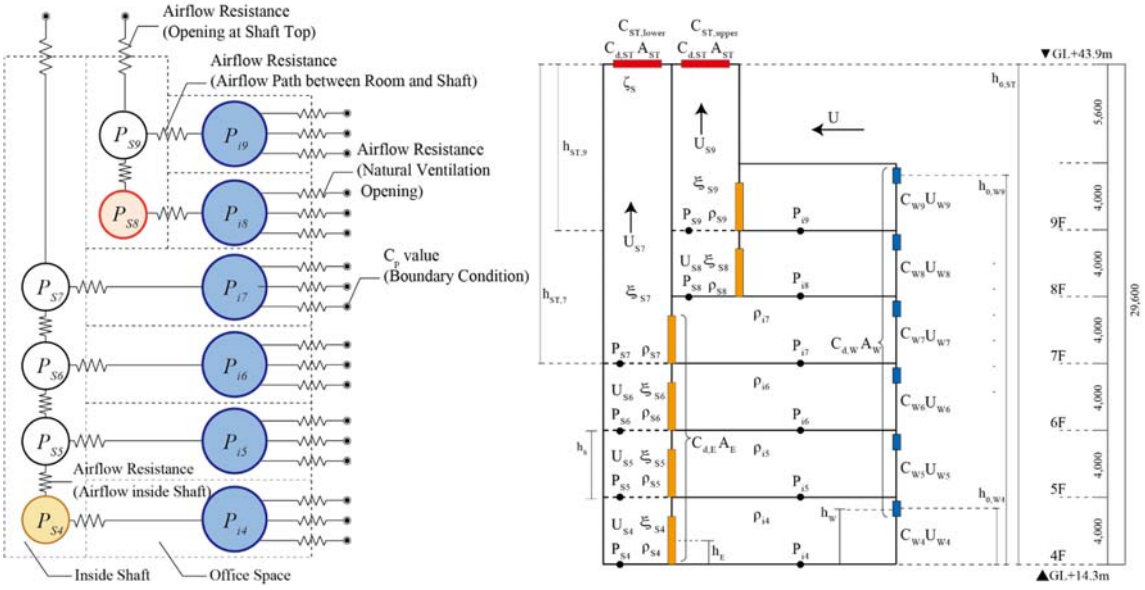

Figure 16: Flow Network Model for Studied Building

damper. $h_{ST,j}$ is the height from 7th or 9th floor to the opening of the shaft top. The pressure loss at each opening is expressed by the following equation.

1) At the NV opening (positive direction is inflow to the room)

$$\Delta P_{Wj} = C_{Wj}\frac{\rho_0}{2}U_{Wj}^2 + (\rho_{ij}h_W - \rho_0 h_{0,Wj})g - P_{ij} \quad (4).$$

2) At the exhaust damper (positive direction is inflow to the shaft)

$$\Delta P_{Ej} = P_{ij} - P_{Sj} + (\rho_{Sj} - \rho_{ij})gh_E \quad (5).$$

3) At the top opening of shaft (positive direction is outflow the shaft)

$$\Delta P_{ST,upper} = P_{S9} + (\rho_0 h_{0,ST} - \rho_{S9}h_{ST,9})g - C_{ST,upper}\frac{\rho_0}{2}U_{ST}^2 - \xi_{S9}\frac{\rho_{S9}}{2}U_{S9}^2$$
$$\Delta P_{ST,lower} = P_{S7} + (\rho_0 h_{0,ST} - \rho_{S7}h_{ST,7})g - C_{ST,lower}\frac{\rho_0}{2}U_{ST}^2 - \xi_{S7}\frac{\rho_{S7}}{2}U_{S7}^2 \quad (6).$$

The pressure loss coefficient due to friction inside the shaft is expressed by the following equation,

$$\xi_{Sj} = \lambda\frac{l_j}{d} \quad (7).$$

where, λ is the friction coefficient of the inner wall surface of the shaft, l_j is the shaft length for each floor, and d is the equivalent diameter of the shaft.

The relationship between the pressures in the divided shafts is expressed by the following equation.

$$P_{S(j+1)} = P_{Sj} - \rho_{Sj}gh_S - \xi_{Sj}\frac{\rho_{Sj}}{2}U_{Sj}^2 \quad (8).$$

Where, h_S is the height of shaft divided for each floor. A function defining the flow direction is defined by the following equation.

$$sign(\Delta P) = \{+1(\Delta P > 0), -1(\Delta P < 0)\} \quad (9).$$

The airflow rate Q is then expressed by;

$$Q = sign(\Delta P)C_d A\sqrt{\frac{2}{\rho}|\Delta P|} \quad (10).$$

where, C_d [-] is the discharge coefficient of each opening and A [m^2] is the opening area. The airflow rate balance (mass conservation) for each room is expressed by;

$$\sum Q_{ij} = 0$$
$$\sum Q_{Sj} = 0 \quad (11).$$

By solving these equations simultaneously, the airflow rate passing through each opening can be obtained.

4.3 Boundary conditions

The flow network calculation was performed by changing the boundary conditions such as the external wind speed and the outside air temperature, and examined the NV characteristics

of the target building. **Table 4** shows the boundary conditions. The external wind speed is the value at the rooftop, the room temperature is 24 °C, the outdoor air temperature is 20 °C assuming the mid-season. The temperature inside the shaft is the average value of the outdoor and room air temperature.

Table 4: Calculation case of flow network model

Boundary Condition	Unit	Standard	Parameter
Outdoor Temperature	°C	20.0	16.0, 20.0, 24.0
Room Temperature		24.0	constant
Wind Velocity(GL+49)	m/s	5.0	0, 3.0, 5.0, 6.0
Wind Direction	-	SE	N, NE, E, SE, S, SW, W, NW

4.4 Results and discussion

Figure 17 shows the results of calculated the airflow rate of each floor for 8 wind direction with the external wind speed changed as a parameter. The radar chart located at the center of the figure shows the airflow rate of the 6th floor for each wind direction, and the others shows the airflow rate of each floor for each wind direction. In all wind directions, the larger the external wind speed is, the larger the absolute value of the airflow rate of each floor becomes. In cases of N and W wind direction, outdoor air flows from the shaft to the room. This is because the wind pressure at the opening of the shaft top is larger than that of NV openings. Under windless condition, where temperature difference is the only driving force of NV, the airflow rate increases at the lower floors where the buoyancy force of the shaft becomes larger. In the cases of wind direction S, SE, and E, the influence of the external wind dominates the buoyancy, and the airflow rate in the upper floor is large.

Figure 18 shows the result of calculated airflow rate, where outdoor air temperature changed as a parameter. The central graph indicates the airflow rate of the 6th floor as well. The airflow rate becomes larger when the temperature difference. Under the condition of no temperature difference, where only the external wind is the driving force, the backflow from the shaft to the room can be seen in the wind direction of N and W. However, in the conditions with the temperature difference, no backflow can be seen. At the lower floor where the buoyancy force of the shaft increases, the airflow rate becomes large. In the wind

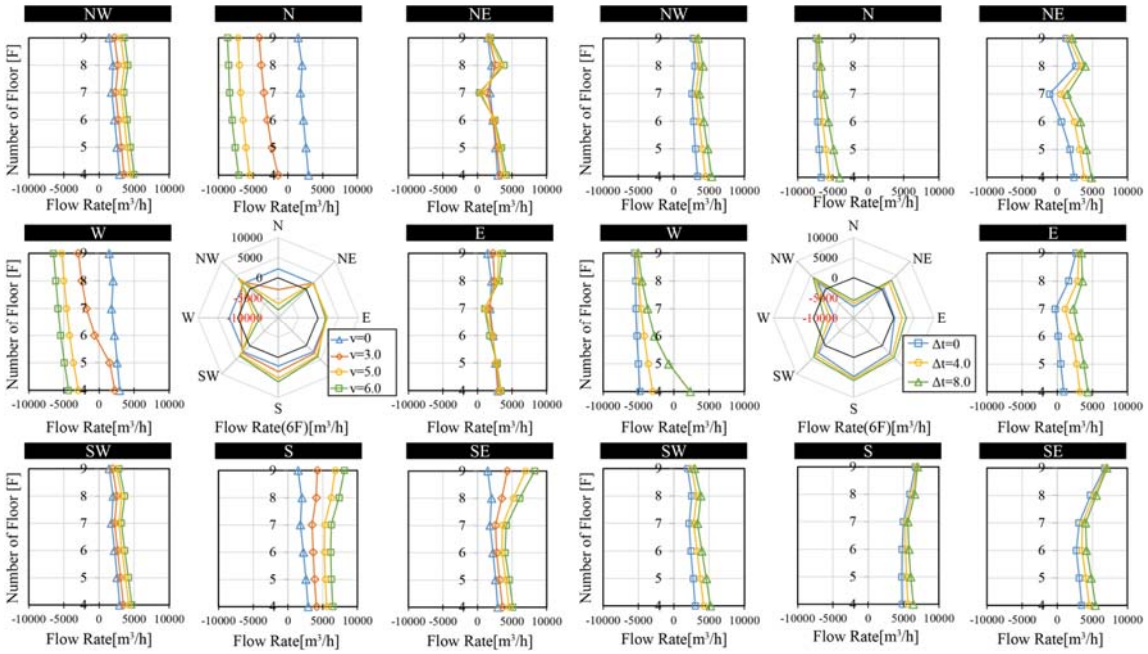

Figure 17: Airflow rate at each floor for each external

Figure 18: Airflow rate at each floor for OA temperature

directions of S, SE, and E, the influence of the wind force is large, and consequently the airflow rate of the upper floor becomes large.

5 CONCLUSION

In this paper, the on-site measurement and flow network calculation was performed for the office building with the NV shaft, and the airflow rate of the target building was obtained. In the on-site measurement, the airflow rate was calculated by a simplified method using occupants' exhaled CO_2 as a tracer gas. The correlation between airflow rate and indoor/outdoor temperature difference, the temperature difference between outdoor and inside the shaft, and the external wind speed was analyzed. As a result, it has been confirmed that the air change rate (ACH) of approximately 1.0 to 2.0 [1/h] could be obtained by opening the NV opening. It was also revealed that in the target building, the influence of indoor/outdoor temperature difference is the largest. The wind pressure coefficient on the wall surface of the target building was obtained by CFD analysis, and flow network calculation was performed under several outdoor conditions. Then, the NV characteristics of the target building was examined by flow network model. As future prospects, we intend to acquire the wind pressure coefficient of the office building in the high-density city block model by wind tunnel experiment for the investigations to establish general NV design method.

6 EXPLANATION OF CHARACTERS

Character	Unit		Character	Unit	
A_W	[m^2]	Area of NV opening	M	[m^3/h]	Amount of CO_2 generated indoors
A_E	[m^2]	Area of exhaust damper	N	[1/h]	Air changes per hour
A_{ST}	[m^2]	Area of shaft top	Q	[m^3/h]	Flow rate
C_{Wj}	[-]	Wind pressure coefficient of NV opening on J-th floor	t_r	[°C]	Indoor temperature
C_{ST}	[-]	Wind pressure coefficient of the shaft top	t_S	[°C]	Temperature inside shaft
C_{t0}	[m^3/m^3]	Indoor CO_2 concentration at the start of measurement	t_0	[°C]	Outside air temperature
C_t	[m^3/m^3]	Indoor CO_2 concentration after t hours	U	[m/s]	External wind speed (at rooftop)
C_0	[m^3/m^3]	Outside air CO_2 concentration	U_{Wj}	[m/s]	External wind speed (at NV opening on J-th floor)
h_S	[m]	Height of shaft divided on each floor	U_{Sj}	[m/s]	Wind speed inside shaft on j-th floor
h_W	[m]	Height from floor level to the NV opening	V	[m^3]	Chamber volume
h_E	[m]	Height from floor level to the exhaust damper	$C_{d,W}$	[-]	Discharge coefficient of NV openings
$h_{0,Wj}$	[m]	Height from the outside air pressure reference height to the natural ventilation openings on j-th floor	$C_{d,E}$	[-]	Discharge coefficient of exhaust damper
$h_{0,ST}$	[m]	Height from the outside air pressure reference height to the shaft top	$C_{d,ST}$	[-]	Discharge coefficient of shaft top
$h_{ST,j}$	[m]	Height from floor level of j-th floor to the shaft top	ξ_S	[-]	Pressure loss coefficient of shaft

7 ACKNOWLEDGEMENTS

The authors deeply appreciate to Hulic Co., Ltd. and undergraduate students of Toyo University for their great cooperation in this research and measurement. Advice and comments given by associate Prof. Kobayashi has been a great help in writing this paper. A part of this work was supported by JSPS KAKENHI Grant Numbers JP17H01308, JP16H04466. Finally, special thanks are due to the late Prof. Hisashi Kotani for kind guidance with enthusiasm.

8 REFERENCES

[1] Kotani H et al.: Natural Ventilation Design Handbook for Architects and Building Engineers, Architectural Institute of Japan, 2016

[2] Hasegawa I, Yamanaka T, Kotani H, Momoi Y, Sagara K, Ochiai N: Study on Natural Ventilation System Combined with Solar Heat and Supplemental Fan for Tenant Office Building (Part1) Character of the Natural Ventilation and Operation Record of the System, Proceedings of Annual Meeting of SHASE, pp.89-92, 2013/09 (In Japanese)

[3] Tajima M, Inoue T, Ohnishi Y: Estimation of Occupants' Carbon Dioxide Production Rate For Measurement of Ventilation J. Environ. Eng., AIJ, No.728,pp.885-892,2016 (In Japanese)

[4] Lim E, Yamanaka T: Development of Zonal Model for Predicting Temperature Distribution inside an Office Room with Hybrid Air-conditioning System, AIVC International Conference 2010

[5] Japan Industrial Standards Committee: JIS A14061974 Room Ventilation Measurement Method (CO_2 Method), 2010